Effect of Side Chains on Competing Pathways for β-Scission Reactions of Peptide-Backbone Alkoxyl Radicals

Geoffrey P. F. Wood,[†,‡] Christopher J. Easton,[‡,§] Arvi Rauk,[⊥] Michael J. Davies,[‡,||] and Leo Radom*[,†,‡]

School of Chemistry, University of Sydney, Sydney, NSW 2006, Australia, Research School of Chemistry, Australian National University, Canberra, ACT 0200, Australia, Department of Chemistry, University of Calgary, Calgary, AB, T2N IN4 Canada, Heart Research Institute, Camperdown, Sydney, NSW 2050, Australia, and ARC Centre of Excellence in Free Radical Chemistry and Biotechnology

Received: May 12, 2006; In Final Form: July 3, 2006

High-level quantum chemistry calculations have been carried out to investigate β-scission reactions of alkoxyl radicals located at the α-carbon of a peptide backbone. This type of alkoxyl radical may undergo three possible β-scission reactions, namely C−C β-scission of the backbone, C−N β-scission of the backbone, and C−R β-scission of the side chain. We find that the rates for the C−C β-scission reactions are all very fast, with rate constants of the order 10^{12} s^{-1} that are essentially independent of the side chain. The C−N β-scission reactions are all slow, with rate constants that range from $10^{-0.7}$ to $10^{-4.5}$ s^{-1}. The rates of the C−R β-scission reactions depend on the side chain and range from moderately fast (10^{7} s^{-1}) to very fast (10^{12} s^{-1}). The rates of the C−R β-scission reactions correlate well with the relative stabilities of the resultant side-chain product radicals (•R), as reflected in calculated radical stabilization energies (RSEs). The order of stabilities for the side-chain fragment radicals for the natural amino acids is found to be Ala < Glu < Gln ∼ Leu ∼ Met ∼ Lys ∼ Arg < Asp ∼ Ile ∼ Asn ∼ Val < Ser ∼ Thr ∼ Cys < Phe ∼ Tyr ∼ His ∼ Trp. We predict that for side-chain C−R β-scission reactions to effectively compete with the backbone C−C β-scission reactions, the side-chain fragment radicals would generally need an RSE greater than ∼30 kJ mol^{-1}. Thus, the residues that may lead to competitive side-chain β-scission reactions are Ser, Thr, Cys, Phe, Tyr, His, and Trp.

1. Introduction

Radical-mediated protein damage has been implicated in a number of diseases such as Alzheimer's disease, atherosclerosis, and diabetes as well as aging.[1,2] Radicals may be formed in biological systems through exogenous processes such as radiation or reactions of toxic chemicals. Alternatively, they can be formed through endogenous processes such as leakage from electron-transport chains and through enzyme-mediated redox reactions.[3] In particular, reactive oxygen species (ROS) have been postulated to react with amino acid residues on both the backbone and the side chains. The resultant radicals are short-lived species and undergo isomerization and fragmentation reactions, leading to the production of further radicals that propagate damage on proteins.[4]

Alkoxyl radicals are a particular class of short-lived ROS that have been postulated to form through initial hydrogen abstractions on alkyl side chains or on the α-carbon of an amino acid residue. Their involvement in radical reactions on proteins has been determined through the detection and characterization of hydroperoxides,[5] from which they can be formed via a tetroxide or via one-electron reduction reactions. It has been established, both through experimental atmospheric and solution chemistry studies and through theoretical computations, that alkoxyl radicals can inter alia undergo three classes of reactions, namely β-scission, skeletal rearrangements, and 1,5-hydrogen shifts.[5b,6] It might be expected that peptide-backbone alkoxyl radicals will undergo the same types of reactions, as shown in reactions 1, 2, and 3, respectively.

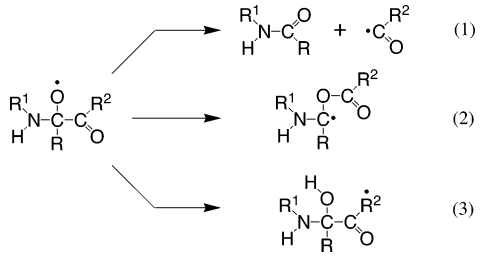

Experimentally, it is difficult to obtain quantitative information on the individual reactions, though some experimental evidence has been obtained for the occurrence of reaction 1.[5b,7] This is because the reactions are fast and can involve chain processes, which makes it problematic to isolate the particular reaction of interest. An additional degree of complexity arises because each of the three classes of reactions can in principle undergo three variations. For example, because there are three different groups joined to the α-carbon, reaction 1 is just one of three possible β-scission reactions that can occur, namely, β-scission of the C−C bond (A), β-scission of the C−N bond (B), or β-scission of the side-chain C−R bond (C):

Previous electron paramagnetic spectroscopy (EPR) spin-trapping studies have suggested that process A predominates, though the occurrence of other reactions could not be discounted.[5b]

* E-mail: radom@chem.usyd.edu.au.
† University of Sydney.
‡ Centre of Excellence in Free Radical Chemistry and Biotechnology.
§ Australian National University.
⊥ University of Calgary.
|| Heart Research Institute.

10.1021/jp062916j CCC: $33.50
Published on Web 08/10/2006

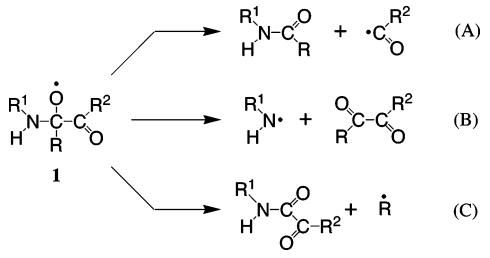

This was confirmed recently for a Gly-containing peptide through product studies.[7] The investigations showed that the α-alkoxyglycyl radical (**3**) derived from α-*tert*-butylperoxy-*N*-benzoylglycine methyl ester (**2**), through either photolysis or reduction with tris-(triphenylphosphine) dichlororuthenium, underwent β-scission of the α-carbon−carbonyl bond to give *N*-formylbenzamide (**4**) in good yield,[7] i.e.,

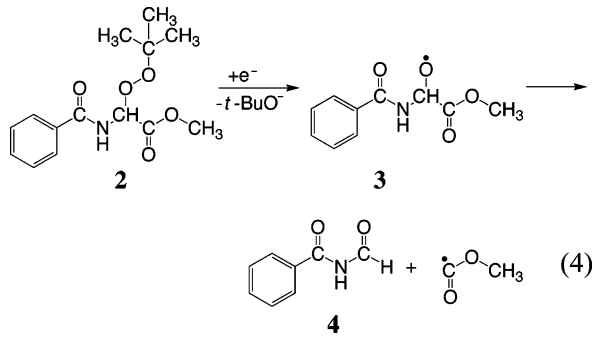

As a first step in understanding the β-scission reactions that can take place in a protein undergoing oxidative stress, we examine in this study which of the three possible β-scission reactions for an α-C alkoxyl radical are most likely to occur. In a preliminary investigation,[8] the three competing pathways were investigated with B3-LYP/6-31G(d) for a model peptide containing either a Gly or an Ala residue. The lowest fragmentation barriers were found for the C−C β-scission pathway A for both residues, in accord with experimental data.[5b,7] The differences in the calculated barriers between pathways A, B, and C for peptides containing a Gly or an Ala residue were sufficiently large that conclusions about the most favorable pathway are likely to hold, despite a subsequent study[9] that showed B3-LYP/6-31G(d) to give results of only moderate accuracy.[10]

In the present study, we examine in more detail the β-scission pathways A, B, and C, first by using higher levels of theory than previously employed on the glycine and alanine peptide models and, second, by examining a wider range of peptide models to see how the thermochemistry and rates of reaction change with the side chain. It has previously been found that the activation energies for β-scission reactions are often determined largely by the stabilities of the daughter radicals.[11] Therefore, we examine whether the large gap previously found[8] between the barriers for C−C (A) and C−R (C) β-scission reactions decreases if the side-chain reactions involve residues that give rise to highly stabilized fragment radicals. We find that the C−R β-scission can indeed become competitive with backbone C−C β-scission in such circumstances. Attempts to test this prediction experimentally have so far proved challenging.

2. Theoretical Methods

Standard ab initio molecular orbital theory[12] and density functional theory (DFT)[13] calculations were carried out with the GAUSSIAN 03[14] and MOLPRO 2002.6[15] computer programs. Except when unrestricted (U) wave functions are required as part of a defined composite method such as CBS-QB3 or G3(MP2)//UB3-LYP (see below), all CCSD(T) calculations were carried out with an unrestricted coupled-cluster procedure based on an RHF starting point (designated URCCSD(T)), as defined in MOLPRO. All remaining calculations were carried out with GAUSSIAN 03, including density functional theory calculations, which used default grid sizes and functional definitions.

In a recent assessment of theoretical methods for the determination of accurate thermochemical properties for C−C β-scission reactions (A) of model peptide-backbone alkoxyl radicals,[9] we identified a number of procedures that would be suitable for such investigations. B3-LYP/6-31G(d)[16] geometries were found to be reliable for single-point energy evaluations with higher levels of theory. For the calculation of enthalpies and barriers, G3(MP2)//UB3-LYP[17] and G3X(MP2)-RAD[18] gave results with an accuracy similar to that of more expensive high-level methods, such as CBS-QB3[19] and W1.[20] Cost-effective alternative procedures included UB3-LYP/6-311+G(3df,2p)//UB3-LYP/6-31G(d), RB3-LYP/6-311+G(3df,2p)//UB3-LYP/6-31G(d), UBMK/6-311+G(3df,2p)//UB3-LYP/6-31G(d), and RBMK/6-311+G(3df,2p)//UB3-LYP/6-31G(d), where BMK is the recently formulated kinetic functional of Boese and Martin.[21] The assessment of theoretical methods is extended in the present study to the C−N β-scission pathway (B) and the C−R β-scission pathway (C). Geometries have been optimized and harmonic frequencies, used to obtain zero-point vibrational energies (with a scale factor of 0.9806[22]), have been calculated using B3-LYP/6-31G(d). Energies were calculated using a selection of the methods noted above to have performed best for pathway A. Radical stabilization energies (RSEs) for radicals •R have been calculated as the energy change in the formal reaction:

$$\bullet R + CH_4 \rightarrow RH + \bullet CH_3$$

i.e., the difference in bond dissociation energies for CH_4 and RH. The RSEs provide a measure of the stabilities of the radicals •R relative to their closed-shell counterparts RH.

Standard transition state theory employing the harmonic approximation[23] was used to obtain Arrhenius parameters (log k, log A, and E_a) at 298 K. We note that all the reactions of the present study are unimolecular, and therefore, the activation energy E_a coincides with $\Delta H^{\ddagger}$, the enthalpy of activation.[24]

Some of the species in the present study have large conformational flexibility, and it is not straightforward to choose geometries that allow consistent comparisons to be made for properties such as enthalpies, barriers, and Arrhenius parameters. For our present purposes, we have chosen geometries in which the backbone of the peptide chain is in an extended-chain conformation. The conformational space of each of the side chains is then explored to find the optimum side-chain configuration. In the calculation of RSEs for the radical fragments resulting from cleavage of the side chain (see below), extended-chain conformations were again used throughout, with the assumption that a major part of the effect of conformation is likely to cancel in a reaction such as $\bullet R + CH_4 \rightarrow RH + \bullet CH_3$.

3. Results and Discussion

3.1. Effect of Level of Theory and Choice of Model on Calculated Reaction Enthalpies and Barriers. In previous work,[9] we examined in detail the effect of the level of theory

on reaction enthalpies and barriers for the C−C β-scission pathway A in models for Ala peptide radicals. A primary conclusion of that study was that large-basis-set calculations with the hybrid density functionals BMK and B3-LYP (either unrestricted or restricted) give reasonable estimates of enthalpies and barriers when compared with high-level composite methods such as W1, G3X(MP2)-RAD, and CBS-QB3.

A notable result was the poor performance of MP2 (with both restricted and unrestricted reference wave functions) for these calculations. This might be associated with the presence of a low-lying excited state in alkoxyl radicals.[9,11] Because the CBS-QB3 and G3X(MP2)-RAD composite methods involve a number of MP2 calculations, the reliability of these methods could be called into question as a consequence of the poor performance of MP2. In this regard, we found in our previous study[9] that the CBS-QB3 and G3-type procedures gave consistent results, which suggests that these procedures *are* giving reliable enthalpies and barriers. However, only a minimal number of external checks were made with high-level procedures (such as W1 and CCSD(T)) that do not involve MP2 calculations. This aspect is therefore examined further here. We also examine the effect of the level of theory on reaction enthalpies and barriers for pathways B and C of an Ala-containing peptide.

3.1.1. C−C β-Scission Reaction (A). Table 1 presents reaction enthalpies and barriers for the C−C β-scission reactions via pathway A, as presented in Figure 1, for six model peptide-backbone alkoxyl radicals. The six reactions have been selected to demonstrate the effect on the thermochemical parameters of building up the peptide chain so as to increasingly simulate the Ala radical center, leading up to the final reaction, which represents our largest model of the peptide backbone (Figure 2). For reactions A1−A3, the CBS-QB3 and G3X(MP2)-RAD results are compared with those of a large-basis-set (cc-pVTZ) URCCSD(T) calculation. The enthalpy and barriers for reaction A1 are also calculated with UBD(T)/cc-pVTZ//UB3-LYP/6-31G(d). In general, the high-level results are in good agreement with one another, suggesting that the basis-set corrections based on MP2 calculations in the case of G3X(MP2)-RAD and the pair-energies extrapolation in CBS-QB3 are not suffering from the same problems in the computation of enthalpies and barriers as does MP2 in isolation. Comparison of the RMP2/6-31G(d) and URCCSD(T)/6-31G(d) reaction enthalpies and β-scission barriers for reactions A1−A4 (Table 1) shows marked differences, whereas the reverse (addition) barriers are in reasonable agreement with one another. This implies a poor performance of MP2 for the reactant alkoxyl radical species, which has been suggested previously[9] and needs to be borne in mind.

In some instances, there is a larger-than-expected difference between CBS-QB3 and G3X(MP2)-RAD. For example, the addition barriers differ by approximately 7−8 kJ mol^{-1} for all four reactions for which a comparison is possible. In these cases, the G3X(MP2)-RAD results tend to be in better agreement with those for the large-basis-set URCCSD(T) and UBD(T) calculations.

As we reported previously,[9] B3-LYP/6-311+G(3df,2p) and BMK/6-311+G(3df,2p) offer cost-effective alternatives for the calculation of reaction enthalpies and barriers. The results in Table 1 suggest that B3-LYP generally underestimates the C−C backbone β-scission barriers while BMK tends to overestimate them. Table 1 also includes MPWB1K/6-311+G(3df,2p) results, which show a more severe overestimation of the β-scission barriers than the other DFT methods when compared with the G3X(MP2)-RAD values. Interestingly, the barriers for the reverse (addition) reactions show less sensitivity to the level of theory.

TABLE 1: Reaction Enthalpies and Barriers (0 K, kJ mol^{-1}) Calculated with Various Theoretical Techniques for Six Model C−C Backbone β-Scission Reactions (A)[a]

reaction[a]	ΔH	$\Delta H^{\ddagger}_{\text{scission}}$	$\Delta H^{\ddagger}_{\text{addition}}$
Reaction A1			
CBS-QB3	3.1[b]	24.4[b]	21.2[b]
G3X(MP2)-RAD	0.4[b]	29.4[b]	29.0[b]
UBD(T)/cc-pVTZ//B3[c]	5.0	32.2	28.7
URCCSD(T)/cc-pVTZ//B3[c]	3.2	32.2	29.0
UB3-LYP/6-311+G(3df,2p)//B3[c]	5.4[b]	23.7[b]	18.2[b]
UBMK/6-311+G(3df,2p)//B3[c]	13.1[b]	35.8[b]	22.6[b]
UMPWB1K/6-311+G(3df,2p)//B3[c]	28.6	48.0	19.3
URCCSD(T)/6-31G(d)	22.4	48.2	25.9
RMP2/6-31G(d)	−6.0	16.1	22.1
Reaction A2			
CBS-QB3	−10.8[b]	19.2[b]	30.0[b]
G3X(MP2)-RAD	−13.6[b]	23.5[b]	37.1[b]
URCCSD(T)/cc-pVTZ//B3[c]	−11.9	24.1	36.1
UB3-LYP/6-311+G(3df,2p)//B3[c]	−14.1[b]	20.4[b]	34.5[b]
UBMK/6-311+G(3df,2p)//B3[c]	−7.2[b]	27.7[b]	34.9[b]
UMPWB1K/6-311+G(3df,2p)//B3[c]	7.5	40.2	32.7
URCCSD(T)/6-31G(d)	8.0	42.8	34.8
RMP2/6-31G(d)	−24.1	5.3	29.4
Reaction A3			
CBS-QB3	15.1[b]	13.9[b]	−1.2[b]
G3X(MP2)-RAD	13.4[b]	19.1[b]	5.6[b]
URCCSD(T)/cc-pVTZ//B3[c]	13.7	19.8	6.0
UB3-LYP/6-311+G(3df,2p)//B3[c]	5.1[b]	14.1[b]	9.3[b]
UBMK/6-311+G(3df,2p)//B3[c]	14.5[b]	22.0[b]	7.5[b]
UMPWB1K/6-311+G(3df,2p)//B3[c]	27.3	30.5	3.2
URCCSD(T)/6-31G(d)	29.7	32.0	2.3
RMP2/6-31G(d)	−3.4	−7.8	−4.4
Reaction A4			
CBS-QB3	−45.8[b]	−4.2[b]	41.6[b]
G3X(MP2)-RAD	−51.9[b]	−2.9[b]	49.1[b]
UB3-LYP/6-311+G(3df,2p)//B3[c]	−60.8[b]	−1.1[b]	59.7[b]
UBMK/6-311+G(3df,2p)//B3[c]	−55.8[b]	3.2[b]	59.1[b]
UMPWB1K/6-311+G(3df,2p)//B3[c]	−45.8	9.1	54.9
URCCSD(T)/6-31G(d)	−40.3	9.9	50.2
RMP2/6-31G(d)	−85.9	−43.7	42.2
Reaction A5			
G3X(MP2)-RAD	−37.4	−0.2	37.6
UB3-LYP/6-311+G(3df,2p)//B3[c]	−31.6	−2.5	34.1
Reaction A6			
UB3-LYP/6-311+G(3df,2p)//B3[c]	−25.0	0.2	24.8

[a] See Figure 1 for details of the reactions. [b] Reference 9. [c] Calculations have been performed on UB3-LYP/6-31G(d) (abbreviated B3) optimized geometries and include scaled (by 0.9806)[22] zero-point vibrational energy.

3.1.2. C−N β-Scission Reaction (B). Table 2 presents reaction enthalpies and barriers for the C−N β-scission reactions via pathway B for the six model peptide-backbone alkoxyl radicals shown in Figure 3. Again, the six reactions have been chosen to incrementally build up the peptide about the radical center in order to increasingly approximate an Ala radical center.

As found previously for pathway A,[9] the high-level composite methods, G3X(MP2)-RAD and CBS-QB3, generally give results in reasonable agreement with one another. Table 2 also includes results with URCCSD(T)/cc-pVTZ//B3-LYP/6-31G(d) for reactions B1−B3 and results with UBD(T)/cc-pVTZ//B3-LYP/6-31G(d) for reactions B1 and B2. The good agreement with the results from the composite methods suggests, as for pathway A (Table 1), that the composite methods do not suffer from problems associated with MP2 calculations. Where there are discrepancies between G3X(MP2)-RAD and CBS-QB3, the

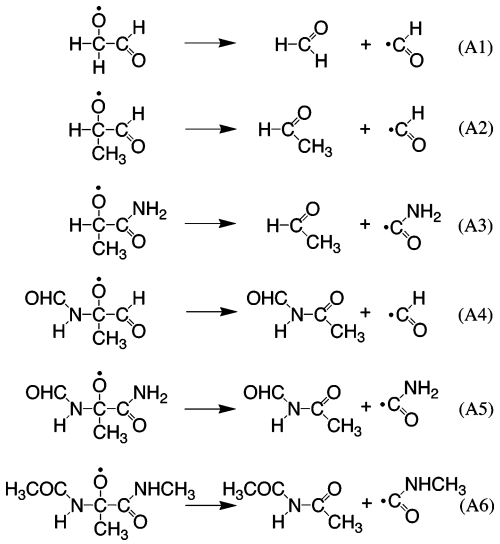

Figure 1. Six model peptides for the study of the β-scission of the C−C backbone bond from an α-C-centered alkoxyl radical.

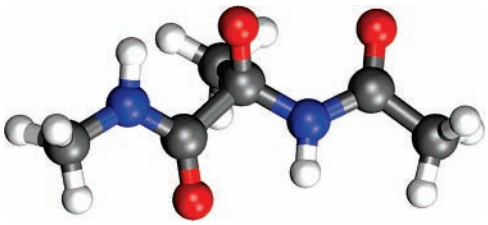

Figure 2. B3-LYP/6-31G(d) optimized structure of the peptide-backbone alkoxyl-radical reactant of reactions A6, B6, and C5 (CH_3-CONH−C(O•)CH_3−CONHCH_3; see Figures 1, 3, and 4), which represents our largest model system.

CCSD(T) and BD(T) results tend to be closer to those obtained from G3X(MP2)-RAD.

The DFT functionals, B3-LYP, BMK, and MPWB1K in association with the 6-311+G(3df,2p) basis set, were also assessed for the calculation of reaction enthalpies and barriers for model peptide-backbone alkoxyl radicals undergoing β-scission via pathway B. As for pathway A, B3-LYP and BMK offer cost-effective alternatives for achieving good accuracy. The results of Table 2 suggest that BMK tends to overestimates β-scission barriers for pathway B as does B3-LYP, albeit to a lesser extent.

3.1.3. C−R β-Scission Reaction (C). Table 3 presents enthalpies and barriers for five peptide-backbone alkoxyl radicals undergoing β-scission via pathway C, as shown in Figure 4. Observations on the sensitivity of the reaction enthalpies and barriers to the level of theory are similar to those made for pathways A and B.

3.1.4. Performance Evaluation. To quantify the observations regarding the performance of the various levels of theory, Table 4 presents the mean absolute deviation (MAD), mean deviation (MD), and largest deviation (LD) from the G3X(MP2)-RAD results for each of these procedures in calculating the reaction enthalpies and barriers for all the reactions of pathways A, B, and C. These statistics indicate that UB3-LYP/6-311+G(3df,-2p)//UB3-LYP/6-31G(d) provides an attractive cost-effective alternative to G3X(MP2)-RAD in the prediction of reaction barriers and enthalpies. The statistics of Table 4 indicate that, at least for the present systems, BMK appears not to perform as well as B3-LYP, in contrast to previous observations.[9]

3.1.5. Model Size Considerations. The results for the model systems of Figures 1, 3, and 4 for each of the pathways A, B, and C provide a means of assessing what system size is suitable for reliably representing the cleavage reactions. It has been noted previously[25] that convergence of calculated RSEs for α-C-centered radicals is achieved once the backbone formally contains an amide functionality on both sides of the radical

TABLE 2: Reaction Enthalpies and Barriers (0 K, kJ mol^{-1}) Calculated with Various Theoretical Techniques for Six Model C−N Backbone β-Scission Reactions (B)[a]

reaction[a]	ΔH	$\Delta H^{\ddagger}_{scission}$	$\Delta H^{\ddagger}_{addition}$
Reaction B1			
CBS-QB3	47.2	59.6	12.3
G3X(MP2)-RAD	42.7	60.4	17.7
UBD(T)/cc-pVTZ//B3[b]	44.7	60.4	15.7
URCCSD(T)/cc-pVTZ//B3[b]	43.9	59.6	15.7
UB3-LYP/6-311+G(3df,2p)//B3[b]	48.1	61.0	12.9
UBMK/6-311+G(3df,2p)//B3[b]	59.0	74.6	15.6
UMPWB1K/6-311+G(3df,2p)//B3[b]	73.1	85.0	11.9
Reaction B2			
CBS-QB3	28.6	46.0	17.4
G3X(MP2)-RAD	21.9	46.1	24.2
UBD(T)/cc-pVTZ//B3[b]	23.3	46.3	23.0
URCCSD(T)/cc-pVTZ//B3[b]	22.2	45.2	23.0
UB3-LYP/6-311+G(3df,2p)//B3[b]	22.8	47.3	24.5
UBMK/6-311+G(3df,2p)//B3[b]	31.5	57.7	26.2
UMPWB1K/6-311+G(3df,2p)//B3[b]	42.9	65.3	22.4
Reaction B3			
CBS-QB3	70.4	90.8	20.4
G3X(MP2)-RAD	66.3	93.5	27.2
URCCSD(T)/cc-pVTZ//B3[b]	65.2	91.5	26.2
UB3-LYP/6-311+G(3df,2p)//B3[b]	56.9	86.9	30.0
UBMK/6-311+G(3df,2p)//B3[b]	72.9	103.2	30.3
UMPWB1K/6-311+G(3df,2p)//B3[b]	88.1	114.9	26.8
Reaction B4			
CBS-QB3	24.5	41.1	16.5
G3X(MP2)-RAD			23.7
UB3-LYP/6-311+G(3df,2p)//B3[b]	10.6	42.3	31.7
UBMK/6-311+G(3df,2p)//B3[b]	19.5	52.9	33.4
UMPWB1K/6-311+G(3df,2p)//B3[b]	29.4	56.0	26.6
Reaction B5			
G3X(MP2)-RAD	56.4	98.4	42.0
UB3-LYP/6-311+G(3df,2p)//B3[b]	43.3	81.8	38.5
Reaction B6			
UB3-LYP/6-311+G(3df,2p)//B3[b]	32.7	82.0	49.3

[a] See Figure 3 for details of the reactions. [b] Calculations have been performed on UB3-LYP/6-31G(d) (abbreviated B3) optimized geometries and include scaled (by 0.9806)[22] zero-point vibrational energy.

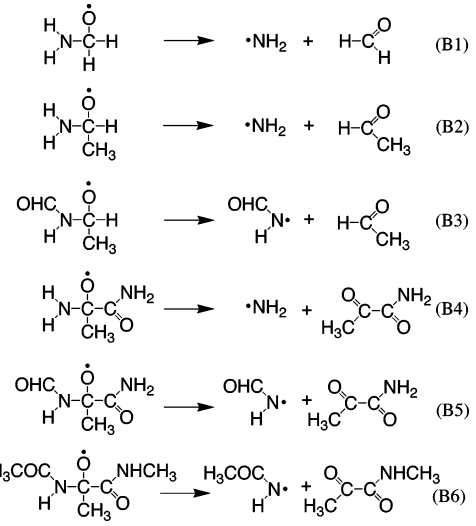

Figure 3. Six model peptides for the study of the β-scission of the C−N backbone bond from an α-C-centered alkoxyl radical.

TABLE 3: Reaction Enthalpies and Barriers (0 K, kJ mol^{-1}) Calculated with Various Theoretical Techniques for Five Model C−R Side-Chain β-Scission Reactions (C)[a]

reaction[a]	ΔH	$\Delta H^{\ddagger}_{\text{scission}}$	$\Delta H^{\ddagger}_{\text{addition}}$
Reaction C1			
CBS-QB3	36.4	61.3	24.9
G3X(MP2)-RAD	32.6	64.3	31.6
UBD(T)/cc-pVTZ//B3[b]	37.0	67.7	30.8
URCCSD(T)/cc-pVTZ//B3[b]	36.1	66.8	30.7
UB3-LYP/6-311+G(3df,2p)//B3[b]	35.2	60.6	25.5
UBMK/6-311+G(3df,2p)//B3	49.1	76.3	27.2
UMPWB1K/6-311+G(3df,2p)//B3[b]	50.7	73.7	23.1
Reaction C2			
CBS-QB3	38.7	52.4	13.8
G3X(MP2)-RAD	33.1	54.1	21.0
URCCSD(T)/cc-pVTZ//B3[b]	35.7	57.0	21.2
UB3-LYP/6-311+G(3df,2p)//B3[b]	38.5	60.0	21.5
UBMK/6-311+G(3df,2p)//B3[b]	47.8	68.0	20.1
UMPWB1K/6-311+G(3df,2p)//B3[b]	60.3	76.6	16.3
Reaction C3			
CBS-QB3	−4.3	37.2	41.5
G3X(MP2)-RAD	−8.9	42.1	50.9
URCCSD(T)/cc-pVTZ//B3[b]	−8.6	42.2	50.8
UB3-LYP/6-311+G(3df,2p)//B3[b]	−15.8	35.1	50.9
UBMK/6-311+G(3df,2p)//B3[b]	−7.8	41.1	48.9
UMPWB1K/6-311+G(3df,2p)//B3[b]	10.4	55.1	44.7
Reaction C4			
G3X(MP2)-RAD	−30.1	29.2	59.3
UB3-LYP/6-311+G(3df,2p)//B3[b]	−29.9	31.9	61.8
UBMK/6-311+G(3df,2p)//B3[b]	−19.8	38.8	58.6
UMPWB1K/6-311+G(3df,2p)//B3[b]	−18.2	36.2	54.4
Reaction C5			
UB3-LYP/6-311+G(3df,2p)//B3[b]	−22.8	38.3	61.1

[a] See Figure 4 for details of the reactions. [b] Calculations have been performed on UB3-LYP/6-31G(d) (abbreviated B3) optimized geometries and include scaled (by 0.9806)[22] zero-point vibrational energy.

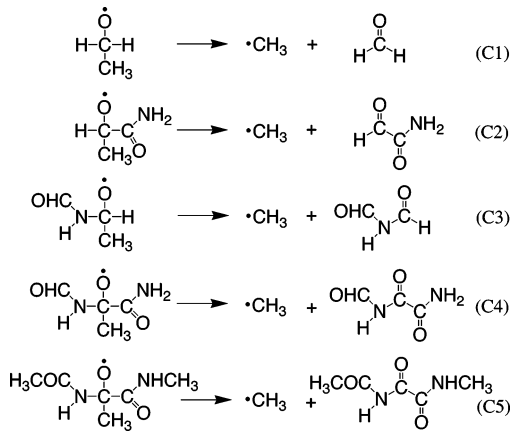

Figure 4. Five model peptides for the study of the β-scission of the C−R side-chain bond from an α-C-centered alkoxyl radical.

center. The results given in Tables 1−3 indicate that the backbone needs to be of *at least* this size to obtain convergence in the enthalpies and barriers for β-scission reactions. The final two reactions in each sequence of models for pathways A, B, and C involve the formal substitution of hydrogen with methyl capping groups. For pathway A, this substitution is accompanied by a small change in the β-scission barrier height (of 2.7 kJ mol^{-1} between A5 and A6 with UB3-LYP/6-311+G(3df,2p)//UB3-LYP/6-31G(d)). The changes in the reaction enthalpy and the addition barrier are slightly greater at 6.6 and 9.3 kJ mol^{-1}, respectively. In an equivalent formal substitution for the models of pathway B, the differences between reactions B5 and B6 are similar: 0.2 kJ mol^{-1} for $\Delta H^{\ddagger}_{\text{scission}}$ and 10.6 and 10.8 kJ mol^{-1} for ΔH and $\Delta H^{\ddagger}_{\text{addition}}$, respectively. For pathway C, the changes in going from reaction C4 to C5 are 6.4, 7.1, and 0.7 kJ mol^{-1} for $\Delta H^{\ddagger}_{\text{scission}}$, ΔH, and $\Delta H^{\ddagger}_{\text{addition}}$, respectively.

TABLE 4: Performance of Various Theoretical Methods for the Calculation of β-Scission Reaction Enthalpies and Barriers[a]

theoretical procedure	ΔH	$\Delta H^{\ddagger}_{\text{scission}}$	$\Delta H^{\ddagger}_{\text{addition}}$
MAD[b]			
CBS-QB3	4.3	2.9	7.2
UB3-LYP/6-311+G(3df,2p)//B3	5.6	4.8	4.0
UBMK/6-311+G(3df,2p)//B3	9.0	8.3	3.2
UMPWB1K/6-311+G(3df,2p)//B3	19.9	16.0	5.0
MD[c]			
CBS-QB3	+4.3	−2.9	−7.2
UB3-LYP/6-311+G(3df,2p)//B3	−2.6	−2.6	−0.4
UBMK/6-311+G(3df,2p)//B3	+8.3	+8.1	−0.2
UMPWB1K/6-311+G(3df,2p)//B3	+19.9	+16.0	−3.9
LD[d]			
CBS-QB3	+6.7	−5.2	−9.4
UB3-LYP/6-311+G(3df,2p)//B3	−13.1	−16.6	−10.8
UBMK/6-311+G(3df,2p)//B3	+16.5	+14.2	+10.0
UMPWB1K/6-311+G(3df,2p)//B3	+30.4	+24.6	−9.7

[a] Calculations have been performed on UB3-LYP/6-31G(d) (abbreviated B3) optimized geometries and include scaled (by 0.9806)[22] zero-point vibrational energy. Energy units are kJ mol^{-1}. [b] Mean absolute deviation from G3X(MP2)-RAD. [c] Mean deviation from G3X(MP2)-RAD. [d] Largest deviation from G3X(MP2)-RAD.

3.1.6. Competing Pathways A, B, and C. The calculations in this section allow us to compare the barriers for the three possible β-scission reactions of peptide-backbone alkoxyl radicals at an Ala residue. These indicate an order of preference A > C > B; this preference for the C−C β-scission pathway A is in accord with previous experimental[5b,7] and theoretical[8] data. For the largest model systems, the thermochemical parameters indicate that the C−C backbone β-scission reaction (A) is essentially barrierless (0.2 kJ mol^{-1}). The β-scission reaction leading to C−CH$_3$ side-chain fragmentation (C) has a higher barrier of 38.3 kJ mol^{-1}, while the C−N backbone β-scission reaction (B) has a still higher barrier (82.0 kJ mol^{-1}).

3.2. Side-Chain Dependence. Our discussion up to now has focused on the β-scission reactions of an alkoxyl radical located at an Ala residue of a peptide. Calculated barriers indicate that pathway A is favored in this case. Experimental product analysis of a Gly containing peptide found that pathway A predominates also for this residue.[7] However, because the rates of β-scission reactions of alkoxyl radicals are sensitively dependent on the stability of the radical that is formed[26] and because more highly stabilized radical products could potentially be formed for other side chains, this may result in the C−R β-scission pathway C becoming competitive with pathway A. To probe these ideas, we begin by examining whether a correlation exists between the calculated radical stabilization energy (RSE) of the fragment radical, on the one hand, and the barriers and enthalpies of the side-chain β-scission reactions of α-C-centered alkoxyl radicals, on the other.

3.2.1. Radical Stabilization Energies. Table 5 shows the radical stabilization energies calculated with G3X(MP2)-RAD of radicals formed from the homolytic bond cleavage of the α-C−R bond, where R is the side chain. The table compares the RSEs for the R groups of all the natural amino acids except for Gly and Pro.

The Ala side-chain fragment radical is •CH$_3$, which has an RSE of zero by definition. The remaining amino acid side chains give RSEs that are all positive, i.e., the radicals are relatively more stable than the •CH$_3$ of alanine. The ordering of RSEs

TABLE 5: Radical Stabilization Energies of Side-Chain Fragment Radicals (•R) Formed from the Homolytic Cleavage of the α-C−R Bond (R = Side Chain) of the Natural Amino Acids[a]

Ala[b]	Glu[c]	Gln[d]	Leu[e]	Met[f]	Lys[g]	Arg[h]	Asp[i]	Ile[j]
0.0	6.1	11.2	11.5	12.8	13.1	13.5	22.4	24.1
Asn[k]	Val[l]	Ser[m]	Thr[n]	Cys[o]	Phe[p]	Tyr[q]	His[r]	Trp[s]
24.4	25.5	33.5	37.3	39.4	59.5	61.5	61.9	62.2

[a] Calculated with G3X(MP2)-RAD at 0 K in units of kJ mol^{-1}. [b] •CH_3. [c] •CH_2CH_2COOH. [d] •$CH_2CH_2CONH_2$. [e] •$CH_2CH(CH_3)_2$. [f] •$CH_2CH_2SCH_3$. [g] •$CH_2CH_2CH_2CH_2NH_2$. [h] •$CH_2CH_2CH_2NHC(NH)NH_2$. [i] •CH_2COOH. [j] •$CH(CH_3)CH_2CH_3$. [k] •CH_2CONH_2. [l] •$CH(CH_3)_2$. [m] •CH_2OH. [n] •$CH(OH)CH_3$. [o] •CH_2SH. [p] •$CH_2-C_6H_5$. [q] •$CH_2-C_6H_4-OH$. [r] •CH_2-imidazole. [s] •CH_2-indole.

for the different R groups is Ala < Glu < Gln ∼ Leu ∼ Met ∼ Lys ∼ Arg < Asp ∼ Ile ∼ Asn ∼ Val < Ser ∼ Thr ∼ Cys < Phe ∼ Tyr ∼ His ∼ Trp.

We expect that the rates of reaction for side-chain cleavage will increase as the RSE of the side-chain fragment increases. To test this hypothesis, we begin by calculating barriers for the three β-scission pathways (A, B, and C) of model systems containing an Ala, Leu, Val, or Phe residue. These residues were chosen to span the range of RSEs given in Table 5, thus providing a sufficient spectrum of enthalpies and barriers so as to give reasonable insights into the side-chain dependence of the reaction rates. We note that preliminary conformational studies of model systems containing other residues such as Asp and Asn showed that intramolecular hydrogen bonding made it difficult to choose an appropriate conformation that represented a realistic protein-bound peptide fragment. This would have hampered a consistent comparison of β-scission enthalpies and barriers. In contrast, the Ala, Leu, Val, and Phe residues all have alkyl side chains that do not make strong internal hydrogen bonds to the backbone amide functionalities.

On the basis of the results of the previous section, the model systems that we use to investigate the β-scission reactions include the backbone that incorporates amide linkages with methyl capping groups formally substituted on each side of the α-C, i.e.,

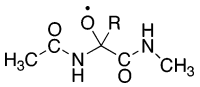

This should represent a reasonable model for estimating rates of reaction in a protein-bound peptide. Unfortunately, this system is already sufficiently large to prevent the use of methods such as G3X(MP2)-RAD with our currently available resources. We have therefore used B3-LYP/6-311+G(3df,2p)//B3-LYP/6-31G(d), which our assessment study suggests should provide a reliable cost-effective alternative to G3X(MP2)-RAD.

3.2.2. Calculated Rate Parameters. Table 6 presents the Arrhenius activation energies (E_a), preexponential factors (given as log A), and rate constants (given as log k) for fragmentation pathways A, B, and C, obtained on the basis of B3-LYP/6-311+G(3df,2p)//B3-LYP/6-31G(d) calculations using the harmonic approximation. Also included are the calculated reaction enthalpies at 0 K (ΔH). The species investigated include model peptides containing an Ala, Leu, Val, or Phe residue.

We note in the first place that the A factors for the three pathways are all very similar, with log A lying between 13.0 and 14.8, which is consistent with results of other theoretical studies of alkoxyl β-scission reactions.[27] Although our calculated rates are only expected to be of moderate accuracy because of the theoretical procedures and peptide models used,[23,28] they do provide insight into the dependence of β-scission rates on residue type. The C−C β-scission rates are all very fast and essentially independent of the nature of the side chain, with log k lying between 11.7 and 13.2. The C−N β-scission rates on the other hand are all very slow. There is a variation in rate constants as a function of side chain of 4 orders of magnitude, with log k ranging from −0.7 to −4.5. The rate constants for the side-chain cleavage pathway C show an even stronger dependence on the residue type, with the rate constant increasing rapidly as the RSE of the side-chain fragment increases. The calculated RSEs provide an approximate basis on which to select residues that are most likely to have competitive C−R β-scission reactions. For Val, the rate of β-scission of the side chain is 1.4 orders of magnitude less than the C−C β-scission reaction of the backbone. Side-chain fragment radicals with RSEs greater than approximately 30 kJ mol^{-1} are likely to have fast side-chain β-scission reactions, with log $k \sim 12 \pm 1$. As the RSE increases above 30 kJ mol^{-1}, it is likely that the side-chain β-scission reaction will increasingly compete with C−C β-scission of the backbone. With an RSE of 59.5 kJ mol^{-1}, the fragment produced from the C−R β-scission reaction of Phe is associated with a side-chain β-scission rate constant that is approximately the same as that for the C−C β-scission reaction. Fragments that have RSEs greater than 59.5 kJ mol^{-1} are expected to provide even stronger candidates for competitive side-chain cleavage. The natural amino acids that give rise to side-chain fragments with calculated RSEs greater than 30 kJ mol^{-1} include Ser, Thr, Cys, Phe, Tyr, His, and Trp. Attempts to provide direct experimental evidence for the theoretical prediction of competitive side-chain cleavage in a manner similar to the approach described by reaction 4 for a Gly-containing peptide have not yet been successful.

TABLE 6: Calculated Arrhenius Parameters and Reaction Enthalpies for the Three Possible β-Scission Reactions of an α-C-Centered Alkoxyl Radical on a Model Peptide Containing Specific Amino Acid Residues[a]

pathway	Ala	Leu	Val	Phe
		C−C β-Scission (A)		
E_a	0.9	11.5	3.7	10.7
log A	14.1	13.7	13.4	13.9
log k	13.2	11.7	12.8	12.0
ΔH	−25.0	−33.7	−31.9	−44.0
		C−N β-Scission (B)		
E_a	85.7	101.1	96.7	89.7
log A	14.8	13.2	13.3	14.4
log k	−0.7	−4.5	−3.7	−1.3
ΔH	32.7	24.4	22.1	49.0
		C−R β-Scission (C)		
E_a	39.5	22.6	9.0	7.7
log A	14.3	13.2	13.0	13.3
log k	6.6	9.3	11.4	11.9
ΔH	−22.8	−45.4	−61.9	−79.8

[a] Calculated within the harmonic approximation at 298 K using UB3-LYP/6-311+G(3df,2p)//UB3-LYP/6-31G(d).

3.2.3. Why Are the C−C β-Scission Reactions Fast? As indicated in the previous section, side-chain fragment radicals that have large RSEs result in C−R β-scission reactions with large rate constants. Similar considerations apply to the C−C β-scission reactions, where the radical product (•$CONHCH_3$) has a large RSE of 37.4 kJ mol^{-1},[29] consistent with the large calculated rates. Significantly smaller rate constants are found for β-scission reactions of non-peptide-related alkoxyl radicals. For instance, in an experimental study of 11 simple alkoxyl radicals,[30] the largest rate constant was found to be ap-

proximately 10^5 s^{-1} for the decomposition of the 2-methyl-2-butoxyl radical ($CH_3CH_2(CH_3)_2CO\bullet$) to give the ethyl radical, consistent with the RSE for the ethyl radical of just 16.3 kJ mol^{-1}.

While the RSE provides a quick and convenient indication of how fast the reaction might go, it is a less direct measure than the reaction enthalpy. The C−C β-scission reactions of the present study are all exothermic, with reaction enthalpies ranging from −25.0 to −44.0 kJ mol^{-1} (see Table 6). This shows that the C−C bond adjacent to the alkoxyl radical is weak and easily ruptured, which is reflected not only in the β-scission rate but also in long reactant bond lengths. For instance, in the model system for Phe, the reactant C−C bond length is 1.606 Å compared with normal C−C lengths of ∼1.54 Å. This can be rationalized in terms of a strong contribution from the nonbonded resonance structure to the overall reactant wave function, i.e.,

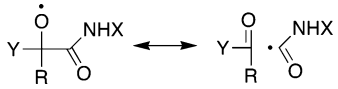

The effect of stabilized radical products on the enthalpy of reaction and hence the rate of reaction can be more clearly seen for the series of C−R β-scission reactions. The rates of these reactions vary by 6 orders of magnitude depending on the stability of the radical that is formed, and follow the reaction enthalpies (−22.8 to −79.8 kJ mol^{-1}; see Table 6) as well as the RSEs (0.0−39.5 kJ mol^{-1}; see Table 5). Again, the larger the rate constant, the weaker the C−R bond and the more easily it is ruptured. This is clearly demonstrated by the progression in the C−R bond lengths for the different residues investigated in this study, i.e., Ala 1.538, Leu 1.583, Val 1.603, and Phe 1.600 Å.

3.2.4. Empirical Rate Relationships. Experimental studies have led to the derivation of empirical relationships to predict Arrhenius parameters of the β-scission reactions of alkoxyl radicals. For example, Choo and Benson[31] have proposed that the activation energy E_a is given by

$$E_a = a + b\Delta H$$

where ΔH is the reaction enthalpy, b is a constant with the value 1.58, and a is a parameter that depends on the ionization energy of the alkyl radical fragment: $a = 8.8 \times \mathrm{IE} - 25.9$, where the IEs are in eV and we have converted all the remaining energy units to kJ mol^{-1}. Since the initial proposal of this equation,[31] improved values for the parameters have been developed by a number of research groups. For example, Atkinson[32] refined the parameters with a larger data set and proposed $a = 10.0 \times \mathrm{IE} - 33.9$ and $b = 0.36$. The large dependence on the ionization energy reflects the tight transition structure with significant polarization,[33] i.e.,

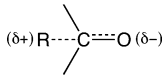

Other researchers have developed structure−activity relationships (SARs) that only depend on the ionization energy of the products[30] or on the nature of the alkoxyl radical.[34]

We have investigated the applicability of a number of these correlations to the alkoxyl radicals of the present study, using theoretical ionization energies (calculated with CBS-QB3) and enthalpies (calculated with UB3-LYP/6-311+G(3df,2p)//UB3-LYP/6-31G(d)). We find that the empirical methods can provide general trends for rate constants but do not describe more subtle differences. This may be a result of the marked differences between the species in the present study compared with those used to derive the SARs. For example, although the empirical activation energies derived from the Atkinson parameters (Table 7) show the general pattern of the calculated values, i.e., high for C−N β-scission reactions and lower for C−C backbone and C−R side-chain β-scission reactions, deviations between the explicitly calculated and empirically estimated activation energies can be large. The best agreement is seen for the C−R side-chain β-scission reactions. This is consistent with the empirical relationships having been derived from data for alkyl-substituted alkoxyl radicals producing alkyl radical fragments. Other more recently derived empirical relationships, which do not involve the reaction enthalpy, have proved to be more accurate in reproducing rate constants for certain sets of cleavage reactions, e.g.,[6d]

$$E_a = 10.46\mathrm{IE} + 8.79n_H - 43.51$$

where the IEs are again in eV, n_H is the number of H atoms attached to the alkoxy carbon, and we have converted all the remaining energy units to kJ mol^{-1}. Unfortunately, relationships of this latter type do not give good absolute agreement with the directly calculated activation energies for the present systems and, in addition, are not suitable for making the subtle distinctions between many of the activation energies because they do not distinguish between different reactions that produce the same fragment radical (Table 7).

TABLE 7: Comparison of Empirical and Directly Calculated Arrhenius Activation Energies (E_a, KJ Mol^{-1})

pathway	IE	E_a(emp)[a]	E_a(emp)[b]	E_a(calc)
		C−C β-Scission (A)		
Ala	6.93	26.7	29.0	0.9
Leu	6.93	23.6	29.0	11.5
Val	6.93	24.2	29.0	3.7
Phe	6.93	19.9	29.0	10.7
		C−N β-Scission (B)		
Ala	9.67	75.0	57.6	84.1
Leu	9.67	72.0	57.6	101.1
Val	9.67	71.1	57.6	96.7
Phe	9.67	80.9	57.6	89.7
		C−R β-Scission (C)		
Ala	9.80	56.3	59.0	39.5
Leu	7.26	22.6	32.4	22.6
Val	7.48	18.9	34.7	9.0
Phe	7.29	10.6	32.8	7.7

[a] Derived from the calculated reaction enthalpy (ΔH, kJ mol^{-1}, Table 6) and the ionization energy (IE, eV) of the radical fragment, using the empirical relationship of Atkinson.[32] [b] Derived from the calculated ionization energy and the number of H atoms attached to the alkoxy carbon, using the empirical relationship of Rayez.[6d]

4. Conclusions

Arrhenius parameters have been calculated for models of the three types of β-scission reactions involving an alkoxyl radical located at the α-carbon position of a peptide. The parameters have been obtained for the Ala, Leu, Val, and Phe residues to illustrate the effect of variation in the side chain. We find that the rates of C−C backbone β-scission are all fast, with rate constants on the order of 10^{12} s^{-1}, consistent with previous EPR data.[5b] The C−N backbone β-scission reactions are all found to have very small rate constants that range from $10^{-4.5}$ to $10^{-0.7}$ s^{-1}. The side-chain C−R β-scission reactions have a range of rate constants that depend on the side chain (R). The rate

constants are found to increase as the stability of the daughter radical (•R) resulting from the side-chain β-scission increases. We predict that alkoxyl radical β-scission reactions from an α-C-centered radical on a peptide involving side-chain daughter radicals that have radical stabilization energies greater than approximately 30 kJ mol^{-1} are likely to compete with the backbone C−C β-scission reaction. The residues identified in this study that are likely to display this behavior include Ser, Thr, Cys, Phe, Tyr, His, and Trp.

Acknowledgment. We gratefully acknowledge funding (to C.J.E., M.J.D., and L.R.) from Australian Research Council Discovery Grants and from the ARC Centre of Excellence in Free Radical Chemistry and Biotechnology, the award (to G.P.F.W.) of an Australian Postgraduate Award, and generous allocations of computing time (to L.R.) from the Australian Partnership for Advanced Computing, the Australian National University Supercomputing Facility, and the Australian Centre for Advanced Computing and Communication.

Supporting Information Available: B3-LYP/6-31G(d) GAUSSIAN archive entries of equilibrium and transition structures are given in Tables S1−S6. This material is available free of charge via the Internet at http://pubs.acs.org.

References and Notes

(1) Davies, M. J.; Dean, R. T. *Radical-Mediated Protein Oxidation: from Chemistry to Medicine*; Oxford University Press: Oxford, New York, 1997, and references therein.

(2) Dean, R. T.; Fu, S.; Stocker, R.; Davies, M. J. *Biochem. J.* **1997**, *324*, 1−18.

(3) Halliwell, B.; Gutteridge, J. M. C. *Free Radicals in Biology and Medicine*; Clarendon Press: Oxford, 1989.

(4) Hawkins, C. L.; Davies, M. J. *Biochim. Biophys. Acta* **2001**, 196−219.

(5) (a) Davies, M. J.; Fu, S.; Dean, R. T. *Biochem. J.* **1995**, *305*, 643−649. (b) Davies, M. J. *Arch. Biochem. Biophys.* **1996**, *336*, 163−172. (c) Gebicki, J. M. *Redox Rep.* **1997**, *3*, 99−110.

(6) See for example: (a) Atkinson, R.; Arey, J. *Chem. Rev.* **2003**, *103*, 4605−4638. (b) Atkinson, R. *Int. J. Chem. Kinet.* **1997**, *29*, 99−111. (c) Mereau, R.; Rayez, M. T.; Caralp, F.; Rayez, J. C. *Phys. Chem. Chem. Phys.* **2000**, *2*, 1919−1928. (d) Mereau, R.; Rayez, M. T.; Caralp, F.; Rayez, J. C. *Phys. Chem. Chem. Phys.* **2000**, *2*, 3765−3772. (e) Devolder, P. *J. Photochem. Photobiol. A* **2003**, *157*, 137−147. (f) Orlando, J. J.; Tyndall, G. S.; Wallington, T. J. *Chem. Rev.* **2003**, *103*, 4657−4689.

(7) Mortimer, A.; Easton, C. J. unpublished data.

(8) Huang, M. L.; Rauk, A. *J. Phys. Org. Chem.* **2004**, *17*, 777−786.

(9) Wood, G. P. F.; Rauk, A.; Radom, L. *J. Chem. Theor. Comput.* **2005**, *1*, 889−899.

(10) In the present study, we find the mean absolute deviation from the G3X(MP2)-RAD values for the reaction enthalpy and barriers for the β-scission reactions A1−A4 (Table 1), B1−B3 (Table 2), and C1−C4 (Table 3) to be 10.9 kJ mol^{-1} with B3-LYP/6-31G(d), which improves to 4.4 kJ mol^{-1} with B3-LYP/6-311+G(3df,2p). See the Supporting Information for full details.

(11) Rauk, A.; Boyd, R. J.; Boyd, S.; Henry, D. J.; Radom, L. *Can. J. Chem.* **2003**, *81*, 431−442.

(12) (a) Hehre, W. J.; Radom, L.; Schleyer, P. v. R.; Pople, J. A. *Ab Initio Molecular Orbital Theory*; Wiley: New York, 1986. (b) Jensen, F. *Introduction to Computational Chemistry*; Wiley: New York, 1999.

(13) Koch, W.; Holthausen, M. C. *A Chemist's Guide to Density Functional Theory*; Wiley-VCH: Weinheim, 2000.

(14) Frisch, M. J.; Trucks, G. W.; Schlegel, H. B.; Scuseria, G. E.; Robb, M. A.; Cheeseman, J. R.; Montgomery, J. A., Jr.; Vreven, T.; Kudin, K. N.; Burant, J. C.; Millam, J. M.; Iyengar, S. S.; Tomasi, J.; Barone, V.; Mennucci, B.; Cossi, M.; Scalmani, G.; Rega, N.; Petersson, G. A.; Nakatsuji, H.; Hada, M.; Ehara, M.; Toyota, K.; Fukuda, R.; Hasegawa, J.; Ishida, M.; Nakajima, T.; Honda, Y.; Kitao, O.; Nakai, H.; Klene, M.; Li, X.; Knox, J. E.; Hratchian, H. P.; Cross, J. B.; Adamo, C.; Jaramillo, J.; Gomperts, R.; Stratmann, R. E.; Yazyev, O.; Austin, A. J.; Cammi, R.; Pomelli, C.; Ochterski, J. W.; Ayala, P. Y.; Morokuma, K.; Voth, G. A.; Salvador, P.; Dannenberg, J. J.; Zakrzewski, V. G.; Dapprich, S.; Daniels, A. D.; Strain, M. C.; Farkas, O.; Malick, D. K.; Rabuck, A. D.; Raghavachari, K.; Foresman, J. B.; Ortiz, J. V.; Cui, Q.; Baboul, A. G.; Clifford, S.; Cioslowski, J.; Stefanov, B. B.; Liu, G.; Liashenko, A.; Piskorz, P.; Komaromi, I.; Martin, R. L.; Fox, D. J.; Keith, T.; Al-Laham, M. A.; Peng, C. Y.; Nanayakkara, A.; Challacombe, M. Gill, P. M. W.; Johnson, B.; Chen, W.; Wong, M. W.; Gonzalez, C.; Pople, J. A. *Gaussian 03*, revision C.02; Gaussian, Inc.; Pittsburgh, PA, 2003.

(15) Werner, H.-J.; Knowles, P. J.; Amos, R. D.; Bernhardsson, A.; Berning, A.; Celani, P.; Cooper, D. L.; Deegan, M. J. O.; Dobbyn, A. J.; Eckert, F.; Hampel, C.; Hetzer, G.; Knowles, P. J.; Korona, T.; Lindh, R.; Lloyd, A. W.; McNicholas, S. J.; Manby, F. R.; Meyer, W.; Mura, M. E.; Nicklass, A.; Palmieri, P.; Pitzer, R.; Rauhut, G.; Schutz, M.; Schumann, U.; Stoll, H.; Stone, A. J.; Tarroni, R.; Thorsteinsson, T. *MOLPRO 2002.6*; University of Birmingham: Birmingham, U.K., 2002.

(16) Becke, A. D. *J. Chem. Phys.* **1993**, *98*, 5648−5652.

(17) Curtiss, L. A.; Redfern, P. C.; Raghavachari, K.; Rassolov, V.; Pople, J. A. *J. Chem. Phys.* **1999**, *110*, 4703−4709.

(18) (a) Henry, D. J.; Parkinson, C. J.; Radom, L. *J. Phys. Chem. A* **2002**, *106*, 7927−7936. (b) Henry, D. J.; Sullivan, M. B.; Radom, L. *J. Chem. Phys.* **2003**, *118*, 4849−4860.

(19) (a) Montgomery, J. A., Jr.; Frisch, M. J.; Ochterski, J. W.; Petersson, G. A. *J. Chem. Phys.* **1999**, *110*, 2822−2827. (b) Montgomery, J. A., Jr.; Frisch, M. J.; Ochterski, J. W.; Petersson, G. A. *J. Chem. Phys.* **2000**, *112*, 6532−6542.

(20) Martin, J. M. L.; De Oliveira, G. J. *J. Chem. Phys.* **1999**, *111*, 1843−1856.

(21) Boese, D. A.; Martin, J. M. L. *J. Chem. Phys.* **2004**, *121*, 3405−3416.

(22) Scott, A. P.; Radom, L. *J. Phys. Chem.* **1996**, *100*, 16502−16513.

(23) For a comparison of Arrhenius parameters obtained using the harmonic approximation with those obtained from a hindered rotor or free rotor treatment, see for example, Gómez-Balderas, R.; Coote, M. L.; Henry, D. J.; Radom, L. *J. Phys. Chem. A* **2004**, *108*, 2874−2883.

(24) Steinfeld, J. I.; Francisco, J. S.; Hase, W. L. *Chemical Kinetics and Dynamics*; Prentice Hall: Englewood Cliffs, NJ, 1989.

(25) Wood, G. P. F.; Moran, D.; Jacob, R.; Radom, L. *J. Phys. Chem. A* **2005**, *109*, 6318−6325.

(26) Gray, P.; Williams, A. *Chem. Rev.* **1959**, *59*, 239−327.

(27) Fittschen, C.; Hippler, H.; Viskolcz, B. *Phys. Chem. Chem. Phys.* **2000**, *2*, 1677−1683.

(28) A variation of approximately 5 kJ mol^{-1} in the activation energy results in a change in the calculated rate constant at 298 K of an order of magnitude. On the basis of the comparison of UB3-LYP/6-311+G(3df,-2p)//UB3-LYP/6-31G(d) results with those of high-level composite methods, we expect our calculated activation energies to have an uncertainty of about ±10 kJ mol^{-1}. Thus, when we refer to our calculated rates as being "moderately accurate", we mean that they should be accurate to within about 2 orders of magnitude. It has previously been found[23] that *A* factors are much less sensitive than E_as to the level of theory used in their calculation. It is therefore the accuracy of the activation energies that is dominant in determining the accuracy of the calculated rates.

(29) The RSE has been determined through G3X(MP2)-RAD calculations, to be consistent with the values of Table 5.

(30) Johnson, D.; Carr, S.; Cox, A. R. *Phys. Chem. Chem. Phys.* **2005**, *7*, 2182−2190.

(31) Choo, K. Y.; Benson, S. W. *Int. J. Chem. Kinet.* **1981**, *13*, 833−844.

(32) Atkinson, R. *Int. J. Chem. Kinet.* **1997**, *29*, 99−111.

(33) A comparison of our calculated UB3-LYP/6-31G(d) natural bond orbital (NBO) charges for the reactant and transition structure of, for example, reaction A6 supports this picture of a polarized transition structure. We find that the oxygen holding the unpaired electron in the reactant has a charge of −0.3, which becomes more negative (−0.6) in the transition structure. In addition, the carbon atom that holds the unpaired electron after the bond breaks has a charge of +0.2 in the reactant, which changes to +0.7 in the transition structure.

(34) Peeters, J.; Fantechi, G.; Vereechken, L. *J. Atmos. Chem.* **2004**, *48*, 59−80.